Photosynthesis Research (2024) 160:31–44
https://doi.org/10.1007/s11120-024-01086-6

RESEARCH

Excitation transfer and quenching in photosystem II, enlightened by carotenoid triplet state in leaves

Agu Laisk[1] · Richard B. Peterson[2] · Vello Oja[1]

Received: 28 September 2023 / Accepted: 6 February 2024 / Published online: 19 March 2024

Abstract

Accumulation of carotenoid (Car) triplet states was investigated by singlet–triplet annihilation, measured as chlorophyll (Chl) fluorescence quenching in sunflower and lettuce leaves. The leaves were illuminated by Xe flashes of 4 µs length at half-height and 525–565 or 410–490 nm spectral band, maximum intensity 2 mol quanta m^{-2} s^{-1}, flash photon dose up to 10 µmol m^{-2} or 4–10 PSII excitations. Superimposed upon the non-photochemically unquenched F_{md} state, fluorescence was strongly quenched near the flash maximum (minimum yield F_e), but returned to the F_{md} level after 30–50 µs. The fraction of PSII containing a ^{3}Car in equilibrium with singlet excitation was calculated as $T_e = (F_{md}—F_e)/F_{md}$. Light dependence of T_e was a rectangular hyperbola, whose initial slope and plateau were determined by the quantum yields of triplet formation and annihilation and by the triplet lifetime. The intrinsic lifetime was 9 µs, but it was strongly shortened by the presence of O_2. The triplet yield was 0.66 without nonphotochemical quenching (NPQ) but approached zero when NP-Quenched fluorescence approached 0.2 F_{md}. The results show that in the F_{md} state a light-adapted charge-separated $PSII_L$ state is formed (Sipka et al., The Plant Cell 33:1286–1302, 2021) in which $Pheo^-P680^+$ radical pair formation is hindered, and excitation is terminated in the antenna by ^{3}Car formation. The results confirm that there is no excitonic connectivity between PSII units. In the $PSII_L$ state each PSII is individually turned into the NPQ state, where excess excitation is quenched in the antenna without ^{3}Car formation.

Keywords Leaves · Triplet states · Photoprotection · Non-photochemical quenching

Abbreviations

Car	Carotenoid
Chl	Chlorophyll
ETC	Electron transport chain
F_o	Fluorescence yield with open centers
F_{md}	During a saturation pulse, without NPQ
F_m	During a saturation pulse, with NPQ
F_f	After a single-turnover flash
F_e	During the maximum quenching by triplets
LED	Light-emitting diode
LHCII	Trimeric light-harvesting complex of PSII
Lhcbm	Monomeric light-harvesting subunit
Lut	Lutein
NPQ	Non-photochemical quenching
PFD, PAD	Photon flux density, incident and absorbed
Pheo	Pheophytin
PSI, PSII	Photosystem I and II
P680	PSII central pigment complex
STFS	Saturating single-turnover flash
Q_A	Primary quinone acceptor of PSII
Q_B	Secondary quinone acceptor of PSII
q_E	Energy-dependent NPQ

Introduction

A principal problem of photosynthesis is termination of excess excitation. It cannot safely occur on a Chl molecule, since with high probability excitations populate the ^{3}Chl↑↑ triplet state (Bowers and Porter 1967), which rapidly exchanges an electron with the natural $^3O_2$↓↓, to form $^1O_2$ ↓↑ and ^{1}Chl↑↓. Preventing singlet oxygen formation is the

Vella Oja: Deceased 20.12.2020.

✉ Agu Laisk
agu.laisk@ut.ee

[1] Institute of Technology, University of Tartu, Nooruse St. 1, 50411 Tartu, Estonia

[2] The Connecticut Agricultural Experiment Station, 123 Huntington St., New Haven, CT 06511, USA

essential task of photoprotective mechanisms (Rutherford et al. 2012).

The photosynthetic electron transport chain contains two photosystems. In PSI, electrons cycle back to the donor side when carriers downstream are fully reduced (Golbeck 1987; Laisk et al. 2007, 2010). Thanks to continuous cycling, in this photosystem electron transfer is rarely blocked by acceptor side reduction, as indicated by low Chl fluorescence from PSI (Schreiber 2023). PSII is not able to rapidly cycle electrons and their transfer stops, leaving the primary acceptor Q_A reduced. The principal difference between the two photosystems is that in PSII excitation remains bound to the antenna while electron transfer is blocked downstream, but in PSI this does not happen. Our recent measurements have shown that, when exposed to a xenon flash, Chl fluorescence yield immediately doubles to the 2 F_o level but keeps rising to the flash F_f level over microseconds: i.e., a time-dependent fluorescence rise is superimposed on the Q_A reduction-dependent fluorescence rise (Christen et al. 1998; Oja and Laisk 2020). This suggests a protein conformation change preventing trapping of excitation in the primary radical pair (Sipka et al. 2021).

A protective mechanism is needed to prevent damage by $^1O_2$ formed from ^{3}Chl when excitation is terminated on Chl. The effective photoprotective mechanism featuring accessory carotenoid pigments—nonphotochemical quenching, NPQ—has been a top theme in photosynthesis research. Carotenoids are present in all pigment-proteins of the photosynthetic machinery. For example, in the trimeric LHCII, each monomer binds 14 chlorophylls, two luteins (Lut1 and Lut2), violaxanthin, and neoxanthin. Carotenoids, such as Lut, possess two excited states in visible light: S_2 generates a wide absorption band near the Soret band of Chl below 500 nm, but the energy level of the S_1 band around 680 nm is close to that of the Chl Q_y transitions. Interestingly, the S_1 band is optically "dark", being "dipole forbidden" for absorbing incident light. The S_1 band can be excited by internal conversion from the S_2 state or by excitation transfer from Chl. The latter has been suggested to be the sole mechanism for NPQ (Ruban et al. 2007): energy is transferred from Chl *a* to the low-lying S_1 (or a nearby S*) excited state of a carotenoid, identified as Chl *a*612/Lut620 (Ballottari et al. 2013; Agostini et al. 2021). The short excited-state lifetime of 10–20 ps (Walla et al. 2000) makes the S_1 band an efficient quencher of excitation.

In this work we show that in leaves, before the onset of NPQ, the high-fluorescent F_{md} state is still protected against $^1O_2$ formation by a mechanism exploiting ^{3}Car triplet formation on the Car-Chl pair. As shown on isolated pigment-protein complexes, the triplet state is rapidly transferred from ^{3}Chl to ^{3}Car in a way that the triplet wavefunction is shared between the carotenoid and the adjacent chlorophyll (Groot et al. 1995; Peterman et al. 1997; Ballottari et al. 2013; Gruber et al. 2015; Gall et al. 2011). As the lowest triplet energy level of carotenoids is below that of $^1O_2$, transfer of the triplet from ^{3}Car to $^3O_2$ is considered impossible (Siefermann-Harms 1987).

Though ^{3}Car formation somewhat shortens the excitation lifetime, this photoprotection only slightly reduces the quantum yield of photochemistry. While in Chl *a* solutions fluorescence lifetime is about 6 ns (Kaplanova and Parma 1984), in detergent solutions the typical lifetime in isolated light-harvesting antenna complexes is 3.5 ns (Pascal et al. 2005; Gruber et al. 2015) and 1–2 ns in the F_{md} state of leaves (Belgio et al. 2012; Holzwarth et al. 2009; Chukhutsina et al. 2019; Farooq et al. 2018). These lifetimes are still much longer than the electron transfer time of about 150 ps, ensuring a high yield of photochemistry (Rutkauskas et al. 2012).

We measured triplet formation and decay in leaves using the property of ^{3}Car to strongly quench ^{1}Chl fluorescence by singlet–triplet annihilation (van Grondelle and Duysens 1980; Mathis et al. 1979; Schödel et al. 1999), as recently reported in intact leaves illuminated by xenon flashes of microseconds duration (Oja and Laisk 2020). We show that in closed PSII units, while NPQ has not yet been developed and fluorescence yield is F_{md}, the excitation-terminating pigment pair involves Car, which quenches excitation by forming the triplet state with a high yield. Each such Car-Chl pair quenches excitation within one antenna, without excitonic connectivity between PSIIs. The ^{3}Car is quenched by atmospheric oxygen via a first-order reaction, whose rate exceeds the intrinsic triplet decay rate. Following exposure to high actinic light, the triplet-forming Chl-Car pair is turned into a non-photochemically quenching state individually in each PSII.

Materials and methods

Measurements were carried out basically as described earlier (Oja and Laisk 2020), except that in the previous work the xenon flashes were applied on leaves in the F_o state under low light, but in this work the leaves were preconditioned in the F_{md} state by applying a 300-ms saturation pulse immediately before the xenon flash. The fluorescence level so obtained was maximal, as time was insufficient to develop NPQ.

Poplar *Populus nigra* L. leaves were excised from a tree growing outdoors. Sunflower *Helianthus annuus* L. plants were grown in a growth chamber (Laisk et al. 2016). Lettuce (*Lactuca sativa*, var. afficione) plants were grown in the commercial greenhouse of Grüne Fee Estonia near Tartu. For better stomatal opening, plants were selected during their fast growth phase at about a half of the harvesting size.

An attached leaf was enclosed in the 30-mm diameter leaf chamber of the dual channel gas system (Laisk and Oja 1998; Laisk et al. 2002). The leaf chamber was equipped with a branched fiber-optic light guide, designed for simultaneous illumination by three light sources and optical measurements by multiple detectors (Oja et al. 2010). At the end of the 300-ms saturation pulse, driving the leaf into the F_{md} state, a xenon flash was fired, providing several excitations for each PSII. Fluorescence yield was measured as the ratio of two signals—one recording fluorescence emission, the other the exciting flash intensity. The flash generated ^{3}Car triplets quenching Chl fluorescence most strongly near the maximum of the flash intensity.

Details of the optical system have been described (Oja and Laisk 2020). Briefly, one illumination branch was connected to a 700 nm LED, providing background far-red light to completely oxidize the ETC and randomize S-states due to weak PSII excitation. Another branch was connected to a 460 nm LED, providing up to 6200 µmol quanta m^{-2} s^{-1} to drive the leaf into the F_m state. Single-turnover flashes were generated by a Machine Vision Strobe MVS7020 (EG&G Optoelectronics, Salem, MA), connected to the third illumination branch. When equipped with a 4 µF discharge capacitor the lamp generated a flash 4 µs wide at the half-height and with a 12 µF capacitor the half-height was 6 µs wide, most energy coming during 10 µs. A much wider flash was shaped by connecting an induction coil between the capacitor and the lamp (Oja and Laisk 2020). The flash profiles were accompanied by a low intensity tail lasting about 40 µs, which was used as "measuring light" to monitor fluorescence yield after the flash had elapsed. The flashes were band-filtered between 525 and 565 or 410–490 nm. Illumination by the green light minimized the intensity gradient across the leaf, but the blue flash provided stronger absorption. The flashlight was measured by calibrated fiber optic spectrophotometer PC2000 (Ocean Optic, Dunedin, FL). The spectra of leaf transmittance, reflectance and absorptance were measured in an integrating sphere (Laisk et al. 2014).

Flash intensity was monitored by recording light reflected from the leaf chamber cover glass and leaf surface. Fluorescence emission was recorded via a 680 nm interference filter (Oja and Laisk 2020). The flash and fluorescence intensity signals were recorded simultaneously by a two-channel oscilloscope LeCroy MSO 64 MXs-B (Chestnut Ridge, NY, USA). The oscilloscope performed one million signal conversions during a flash, which were averaged by groups of 500, recording 2000 data points per flash.

Oxygen evolution was measured in a flow-through system (Laisk and Oja 1998; Laisk et al. 2002) with a zirconium O_2 analyzer (S-3A, Ametek, Pittsburgh, PA, USA) on a background of 10–20 ppm O_2 in N_2 and 200 ppm CO_2 as described earlier (Oja and Laisk 2000; Oja et al. 2011; Laisk et al. 2012; Laisk and Oja 2020). With randomized S-states, $4{\cdot}O_2$ evolution represented integral PSII electron transport during a flash.

Results

During a xenon flash superimposed on the fluorescence saturation pulse in the F_{md} state, fluorescence yield temporarily declined but returned to the F_{md} level after the flash (Fig. 1). Fluorescence quenching was stronger the more intense the flash (Fig. 1b). As the xenon flash is not rectangular but bell-shaped, cumulative photon dose is plotted on the abscissa for convenient further analysis (Fig. 1c).

Triplets in equilibrium with light

The light and oxygen dependence of the flash-induced fluorescence quenching suggests its basis is singlet–triplet annihilation of ^{1}Chl by ^{3}Car (van Grondelle and Duysens 1980; Mathis et al. 1979; Schödel et al. 1999). The fraction of PSII units containing ^{3}Car in the antenna is successfully described by the following budget equation, stating that triplet states are formed by singlet excitations in PSII not containing a triplet, and decay by singlet–triplet annihilation and an intrinsic first-order reaction in PSII containing a triplet:

$$\frac{dT}{dt} = aIS - bIT - cT, \tag{1}$$

where T is the fraction of PSII containing a triplet, $S = 1$—T is the fraction not containing a triplet, I is light intensity (µmol m^{-2} $µs^{-1}$ = mol m^{-2} s^{-1}, we prefer to count time in µs, the unit characteristic of the triplet decay rate); a, and b, m^2 $µmol^{-1}$, are the optical (functional) cross-sections of a µmol of PSII units: a, for triplet formation ($1/a$ is the number of photons, µmol m^{-2}, necessary to generate a triplet in each PSII unit—i.e., to quench fluorescence to zero) and b, for triplet annihilation ($1/b$ is the number of photons, µmol m^{-2}, necessary to annihilate the triplet in each PSII); c is the triplet decay rate constant ($µs^{-1}$). As triplet decay is enhanced by atmospheric oxygen, we present the corresponding rate constant in two parts:

$$c = k_{O2}[O_2] + k_i, \tag{2}$$

where the subscript i denotes the intrinsic decay by intersystem crossing and the first term denotes the O_2-enhanced rate constant for intersystem crossing.

According to Eq. 1, changes in the relative content of triplets, T, lag behind changes in the flashlight intensity I: during the initial, accumulation phase there are fewer,

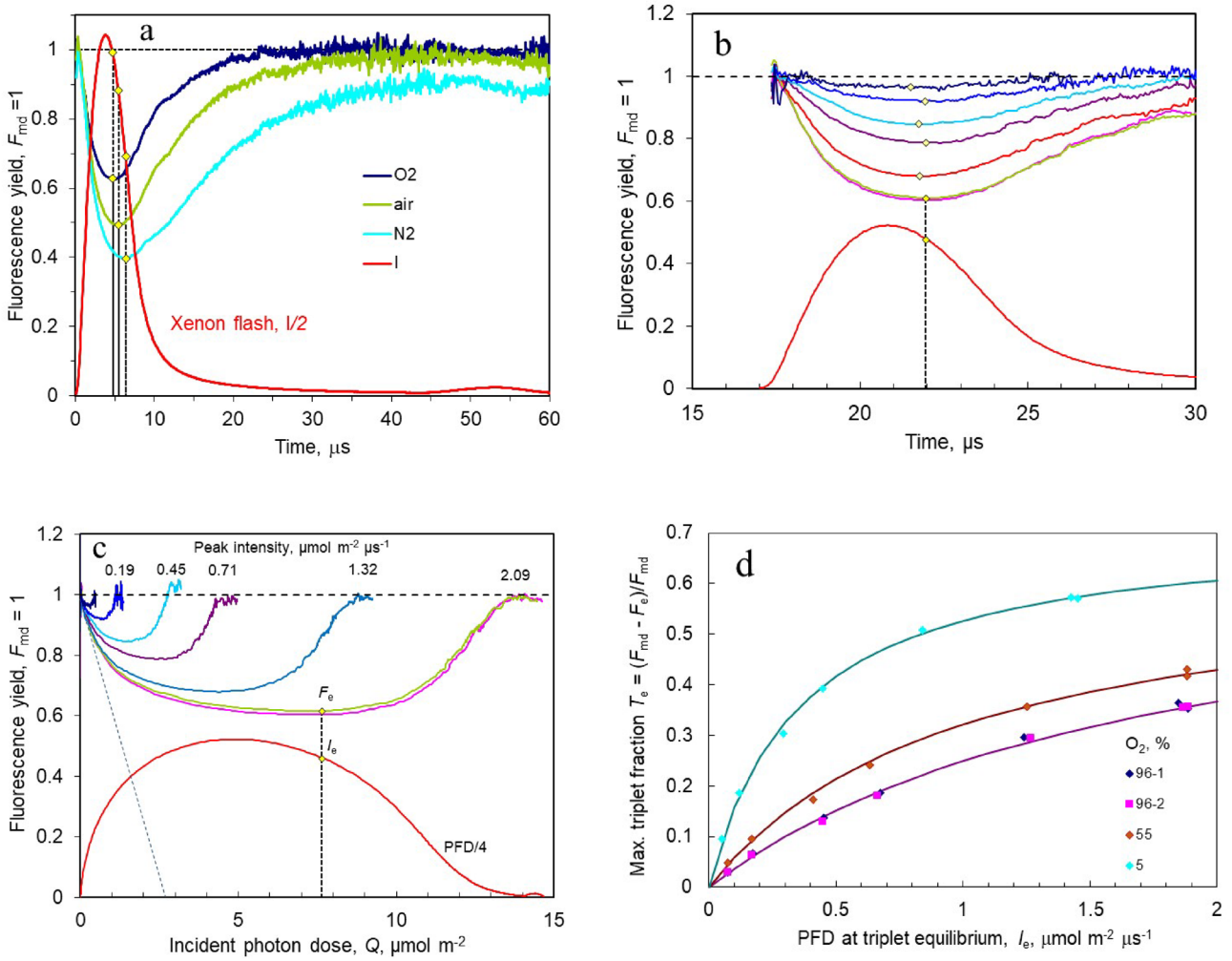

Fig. 1 Measurement of triplet accumulation in leaves. The leaves were pre-adapted for 15 min under 60 µmol m^{-2} s^{-1} of 700 nm LED light, then a 0.3 s saturation pulse of 6200 µmol m^{-2} s^{-1} from a 460 nm LED was applied, to reach the F_{md} state. Finally, a band-filtered Xe flash (410–490 nm) was superimposed (red line, scale on the left axis, µmol m^{-2} μs^{-1}). Chl fluorescence emission f was recorded at 680 nm and the yield $F = f/I$ was calculated. **a** Poplar leaf; oxygen concentration was 0% (blue), 21% (green) and 100% (navy blue); data points joined with vertical lines indicate fluorescence and light intensity values used for equilibrium analysis. **b** Sunflower leaf; the leaf was brought into the F_{md} state as in **a**, then blue flashes of different power were applied and fluorescence yield recorded. The flashlight intensity was (from the top) 0.08, 0.19, 0.45, 0.71, 1.32 and 2.09 µmol m^{-2} μs^{-1} at the peak (the maximum intensity was used twice, as the first and the last of the series); enlarged data points at the minimum fluorescence yield were used for triplet equilibrium analysis; oxygen concentration was 96% in this measurement. **c** Fluorescence yield F and flashlight intensity, I, from **b** are plotted against cumulative dose, Q, µmol photons m^{-2}; flashes of different peak intensity (shown at the curves) provided different full doses, indicated as the abscissa value at the end of each trace. Fraction of PSII containing a ^{3}Car triplet state in equilibrium with light intensity was calculated as $T_e = (F_{md} - F_e)/F_{md}$ (an example shown for the strongest flash); initial slope of the triplet-induced fluorescence quenching extrapolates to the photon requirement of 2.7 µmol m^{-2} for triplet formation in all PSII (dotted line). **d** Triplet fraction T_e in equilibrium with light intensity I_e; measurements of panels **b** and **c** were carried out at different O_2 concentrations, beginning, and ending with 96%. Lines were calculated from Eq. 3

and during the final decay phase there are more, triplets than would have been in equilibrium with a constant light intensity I (t) at time t. At maximum triplet content (minimum fluorescence, F_e) the fraction of PSII containing a triplet is momentarily in equilibrium with light intensity, I_e. Thus, at this moment triplet formation and decay rates are equal so that $dT/dt = 0$ in Eq. 1.

At equilibrium, Eq. 1 yields a hyperbolic function for the triplet content:

$$T_e = \frac{aI_e}{(a+b)I_e + c}. \quad (3)$$

Pairs of values of light intensity, I_e, and the corresponding fraction of PSII containing a triplet, T_e, from the experiment of Fig. 1c, are plotted in Fig. 1d. The lines were calculated from Eq. 3, after properly setting the rate constants.

The rate constants were extracted from the hyperbolic relationships of Fig. 1d after the rate constant for intrinsic decay, k_i (Eq. 2), was measured separately. A strong short flash was applied upon the F_{md} level, but the generated triplets were not measured during the actinic flash. A chase flash was applied after the time interval indicated on the abscissa of Fig. 2. Fluorescence yield was measured with the low excitation intensity in the beginning of the chase flash. Thus, only the decaying tail of the triplet states, generated mainly at the peak of the actinic flash, was measured within the time range of 60 to 80 µs. Notwithstanding the difficult experimental conditions, an exponential decay with the time constant of 9 µs ($k_i = 0.11$ µs^{-1}) was measured (Fig. 2). This lifetime is basic information, showing that the investigated fluorescence quenching was caused by the carotenoid, not chlorophyll, triplet state.

The rate constants a and k_{O2} were found from the measured initial slope of the curves in Fig. 1d. The initial slope of the hyperbolae, $dT_e/dI_e = a/c$, is determined by the optical cross-section a and the decay constant c—in the latter the unknown part is k_{O2} now (Eq. 2). Using the measured initial slope values at 5% and 96% O_2 a system of the following two equations was compiled:

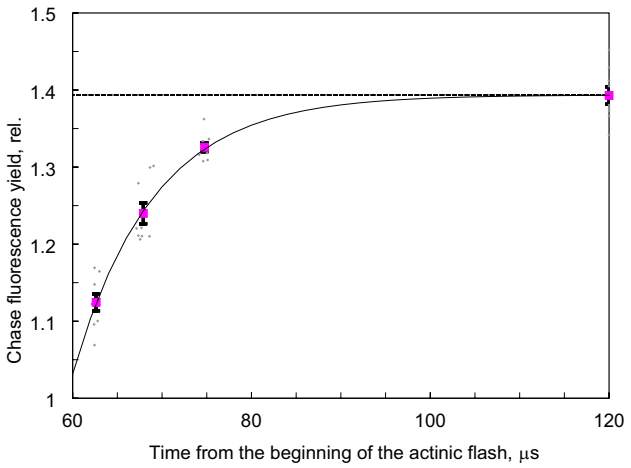

Fig. 2 Measurement of triplet lifetime at 0% O_2 in sunflower. Triplets were generated by a blue actinic flash like in Fig. 1. A chase flash was applied after the time interval indicated on the abscissa. Fluorescence yield was measured with the low excitation intensity in the beginning of the chase flash (each data point is an average of nine measurements, bars indicate standard error). The line is an exponential with the time constant of 9 µs, approaching F_{md}

at 96% O_2, $a = 0.388 \cdot (0.11 + 96ko_2)$,

at 5% O_2, $a = 2.0 \cdot (0.11 + 5ko_2)$,

where the factors before parentheses are the measured dT_e/dI_e values from Fig. 1d. The system solves with $a = 0.285$ m^2 µmol^{-1} and $k_{O2} = 0.0065$ (s^{-1} per % O_2). The latter value quantifies the rate of reaction between the atmospheric O_2 and ^{3}Car in leaves: at 17% O_2 the triplet quenching rate doubles, and at 100% O_2 the rate is six times faster than the intrinsic rate in the absence of oxygen. The cross-section area $a = 0.285$ m^2 µmol^{-1} indicates that $1/0.285 = 3.5$ µmol m^{-2} incident flash photons are required to generate a ^{3}Car triplet in each PSII. Roughly evaluating, about 85% of the blue flashlight photons are absorbed by the leaf, and about half of these photons are exciting PSII. If these 1.5 µmol photons m^{-2} generate triplets in 1 µmol PSII m^{-2}, the quantum yield would be $1/1.5 = 0.66$. The remainder of the energy is partitioned to internal conversion (24%) and fluorescence (10%). This exercise shows that leaf absorptance, excitation partitioning, and density of PSII must be known for meaningful analysis of triplet formation.

Nevertheless, an interesting discrepancy arises by comparing the areas a and b, detectable from the maximum triplet fraction, T_{em}, at saturating light intensity. Though in our experiments the available flash intensities were below saturation at high O_2 concentrations, the hyperbolic model (Eq. 3) predicts all the curves in Fig. 1d approach the same plateau, $T_{em} = a/(a+b) = 0.71$. Knowing a, we obtain $b = 0.116$ and $b/a = 0.4$, which means that while a ^{3}Car triplet is quenching singlet excitation, in less than half of these cases it annihilates itself. Though the plateau of $T_{em} = 0.71$ was extrapolated from the hyperbolic relationships of Fig. 1d, it is clear the 5% O_2 curve exceeds the critical value of $T_{em} = 0.5$-expected if every singlet quenching is accompanied by triplet annihilation—but in no case does it approach the value of $T_{em} = 1.0$-expected if the triplet does not annihilate while quenching the singlet.

Dynamics of triplet formation and decay

The functional cross-section of triplet formation is accessible via the initial slope of the fluorescence traces (Fig. 1c): $dT/dt = aI$ when $T = 0$ (and $S = 1$, Eq. 1). As $dT/dt = dT/dQ \cdot dQ/dt$ and $I = dQ/dt$, we obtain $dT/dQ = a$. The straight line based on the initial slope of the fluorescence curves crosses the axis of abscissa at $1/a = 2.7$ µmol m^{-2}, yielding $a = 0.37$ m^{-2} µmol^{-1}. From the initial slope of the equilibrium curves (Fig. 1d) the yield was 0.29 m^2 µmol^{-1}. Such a big difference between the cross-sectional areas calculated from the equilibrium state and the initial rate

of the triplet-induced fluorescence quenching is a warning about serious limitations in our experimental setup. These values characterize the number of incident photons necessary to generate a triplet state in each PSII unit, based on fluorescence visible to our instrument. Gradients across the leaf in flashlight absorption and fluorescence re-absorption strongly interfere with these estimations.

In the following experiment we related triplet formation to photochemical charge separation in PSII, both indicated by Chl fluorescence and therefore similarly influenced by leaf optical thickness. The PSII photochemical quantum yield was estimated from Chl fluorescence induction during a weaker but longer flash, avoiding triplet accumulation. For this experiment, the charge energy of the 12 µF capacitor, usually converted into the flashlight during about 10 µs, was discharged over a longer time by connecting an induction coil between the capacitor and the xenon tube. As a result, the flash extended to 160 µs, decaying about exponentially. Most of the flash photons were generated during 100 µs—a time short enough to assume minimal $Q_A \rightarrow Q_B$ electron transfer. Different flash intensities were used to maximize Q_A reduction on one hand but keeping triplet accumulation minimal on the other (Fig. 3). The initial slope of the fluorescence induction transient indicated a requirement of 2.5 µmol photons m^{-2} to reach the maximum flash fluorescence level $F_f = 0.54\ F_{md}$. For comparison, from

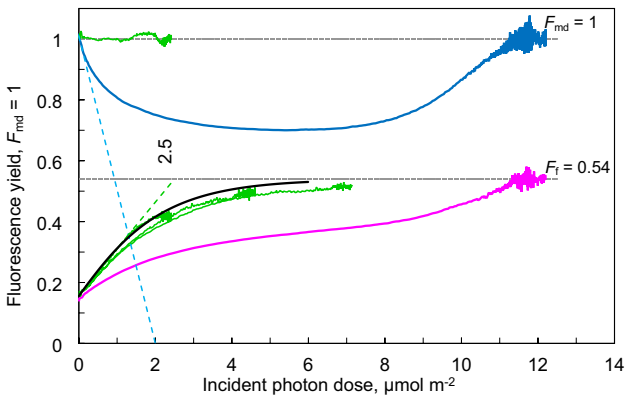

Fig. 3 Comparison of quantum requirements for triplet formation and for photochemical electron transfer. Fluorescence yield (continuous blue) was quenched in a sunflower leaf down from the $F_{md} = 1$ state by triplets generated by a 6 µs-long standard flash. Initial slope of the fluorescence quenching extrapolates to zero at the quantum requirement of 2 µmol m^{-2} (dashed light-blue line). Extended-length flashes generating few triplets were applied on open PSII (three flashes of increasing power, green lines). Their initial slope extrapolates to the requirement of 2.5 µmol photons m^{-2} to reach the flash fluorescence yield F_f (dashed green line). Black line is drawn with the initial slope of the weakest flash and the maximum neglecting triplets. The green line at $F_{md} = 1$ is the weak flash superimposed on the F_{md} state to show that no triplets were generated. The violet line was recorded with the standard 6 µs flash. Note the saturating flash-fluorescence yield $F_f = 0.54\ F_{md}$

the standard flash applied on F_{md} the quantum requirement for triplet formation was 2 µmol m^{-2} in this leaf. According to this result, obtained with the two spectrally similar flashes, the quantum yield of triplet formation in the F_{md} state was not lower, but rather was higher than the quantum yield of PSII charge transfer in the F_o state. Note that during the strong short flash applied in the F_o state, the initial slope of fluorescence induction was by half slower than during the retarded flashes, though triplets had not yet accumulated in both cases. This confirms the microseconds-dependent fluorescence rise, interpreted to show protein conformation change leading to isolation of the PSII reaction center from the antenna (Oja and Laisk 2020). During the short flash triplets accumulated later, quenching about the same per cent of F_f fluorescence as when the same flash was applied on the F_{md} state.

So far, the yield measurements have been related to the dose of photons incident to optically thick leaves of unknown PSII content, resulting in the optical cross-section of the investigated process. A more meaningful value is the quantum yield of triplet formation in an individual PSII unit. In the following experiments we measured the absorbed photon dose and minimized the gradients using pale green lettuce leaves illuminated by green-filtered xenon flashes (Oja and Laisk 2020). Not only the equilibrium data point was analyzed from each measured trace, but the whole trace was mathematically modeled. To simulate leaf optical gradients—e.g. limited visibility of the fluoresced red light—the model was solved separately for 20 sublayers of the leaf cross-section, for which the actinic green light absorption and red fluorescence light visibility were described by exponentials (Oja and Laisk 2020). The leaf response was calculated as the sum of the layer's responses. For the layers, components of the triplet budget were varied, to find the best fit between the modeled response and the experiment result for the whole leaf.

In principle, the dynamic model is the numeric solution of the time-dependent differential Eq. 1. For the bell shape of the xenon flashes, light intensity was calculated as the time-dependent increase (derivative) of the cumulative photon dose per PSII. To do this, the photon dose step dQ per time step dt (flashlight intensity) was calculated from the shape of the flash and substituted for I in the numeric solution. For convenient fitting to the fluorescence traces in Fig. 4 the differential equation was numerically solved in Microsoft Excel for the singlet fraction:

$$S_{i+1} = S_i - S_i \cdot a \cdot Q_{II} \cdot \left(q_{i+1} - q_i\right) + \left(1 - S_i\right) \cdot \left(c \cdot dt + b \cdot Q_{II} \cdot \left(q_{i+1} - q_i\right)\right). \quad (4)$$

Here $Q_{II} = s_{II} \cdot A \cdot Q / n_{II}$ is the total flash dose of excitations per PSII unit, where Q is the incident flash dose, A is leaf

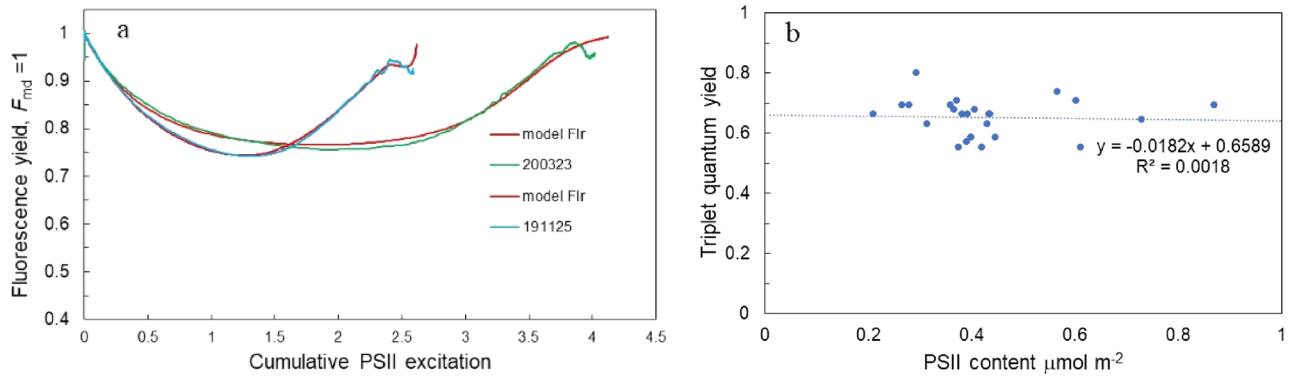

Fig. 4 Modeling of fluorescence traces measured by green-filtered flashing of lettuce leaves. **a** Two example experiments (indicated *yymmdd*). Experiment 200323 (green line) was carried out at O_2 concentration of 60% with incident flash dose of 6.05 μmol quanta m^{-2}, leaf absorption coefficient $A = 0.309$, PSII content 0.31 μmol m^{-2}. The red model line was calculated with the quantum yield for triplet formation $a = 0.62$ and the singlet–triplet annihilation yield $b = 1.0$, triplet lifetime $\tau = 1/c = 2$ μs. Experiment 191125 was carried out at O_2 concentration of 2% with incident flash dose of 4.12 μmol quanta m^{-2}; $A = 0.347$, PSII = 0.39 μmol m^{-2}. The model line was calculated with $a = 0.55$ and $b = 1.0$. **b** Quantum yield of triplet formation per PSII excitation in lettuce leaves with different PSII content, measured during plant growth

absorptance, s_{II} is the partitioning fraction of excitation to PSII and n_{II} is PSII density per m^2, measured from the flash O_2 evolution. Other denotations in Eq. 4: q is the fraction of the flash dose absorbed between the steps i and i + 1, a is now the quantum yield of triplet formation per PSII excitation, b is the quantum yield of triplet annihilation while quenching singlet excitation, c is the rate constant of the triplet state decay, dt is the integration time step (usually 0.05 μs), i is the number of time-steps. Two examples of the fitting quality are shown in Fig. 4a. The initial slope of the rising fluorescence quenching is fitted by varying the quantum yield of triplet formation, a. The maximum degree of quenching is mainly determined by the flash dose, Q, quantum yield of triplet annihilation, b, and to some extent by triplet lifetime, $\tau = 1/c$. The final decay rate is mainly determined by triplet lifetime, which strongly depends on O_2 concentration (Eq. 2).

Such fluorescence traces were measured and modeled in growing lettuce plants, exhibiting gradually greener leaves with rising PSII density. The fitted quantum yield of triplet formation, $a = 0.65$ was practically independent of the PSII density (Fig. 4b). While the model parameters, leaf absorption coefficient and PSII density, were measured, the relative excitation partitioning to PSII, s_{II}, was a free parameter. We started the fitting, setting $s_{II} = 1$. This resulted in low quantum yields—for triplet formation $a = 0.39$ and for triplet annihilation $b = 0.6$. Decreasing the fraction of the PSII light to $s_{II} = 0.6$ (Laisk et al. 2014) increased the annihilation yield to $b = 1$ and the triplet formation yield to $a = 0.65$, not changing the triplet lifetime τ.

Triplet states during non-photochemical quenching

In this section we related the triplet fraction to singlet excitation, this time varied not by changing the flashlight intensity but by adjusting the degree of non-photochemical quenching (NPQ). Triplet measurements were carried out with blue xenon flashes, superimposed on F_m saturation pulses, applied periodically during relaxation of pre-induced NPQ. The direction was chosen to minimize the NPQ gradient over the leaf cross-section: we assumed that once induced completely in all mesophyll cells, under low light NPQ relaxes uniformly in all cells. Relaxation of F_m quenching started with an initial exponential time constant of 3 min, but soon it slowed, passing the half-way point at 5 min, while 40 min were required to approach the initial unquenched F_{md} level. Typical fluorescence signal traces during the xenon flashes are shown for O_2 concentration of 2.5%, plotted against the cumulative photon dose (Fig. 5a). Temporal sequence of the traces begins with the bottom curve, measured right at the end of the q_E-inducing illumination. At the beginning of the flash the fluorescence yield was 0.25 F_{md}, it decreased very little by triplet formation. Flashes given later during the relaxation of NPQ begin at higher F_m but fall deeper due to the triplet-induced quenching. For each curve the equilibrium triplet level was calculated as $T_e = (F_m - F_e)/F_m$, where subscript e indicates fluorescence signal at the minimum (equilibrium between triplet formation and destruction) and F_m is the fluorescence signal at the beginning of the trace. In Fig. 5b these T_e values are plotted versus the fluorescence signal f_e as NPQ relaxed at different O_2 concentrations.

For comparison, the equilibrium triplet level was measured by regulating flash intensity in the absence of

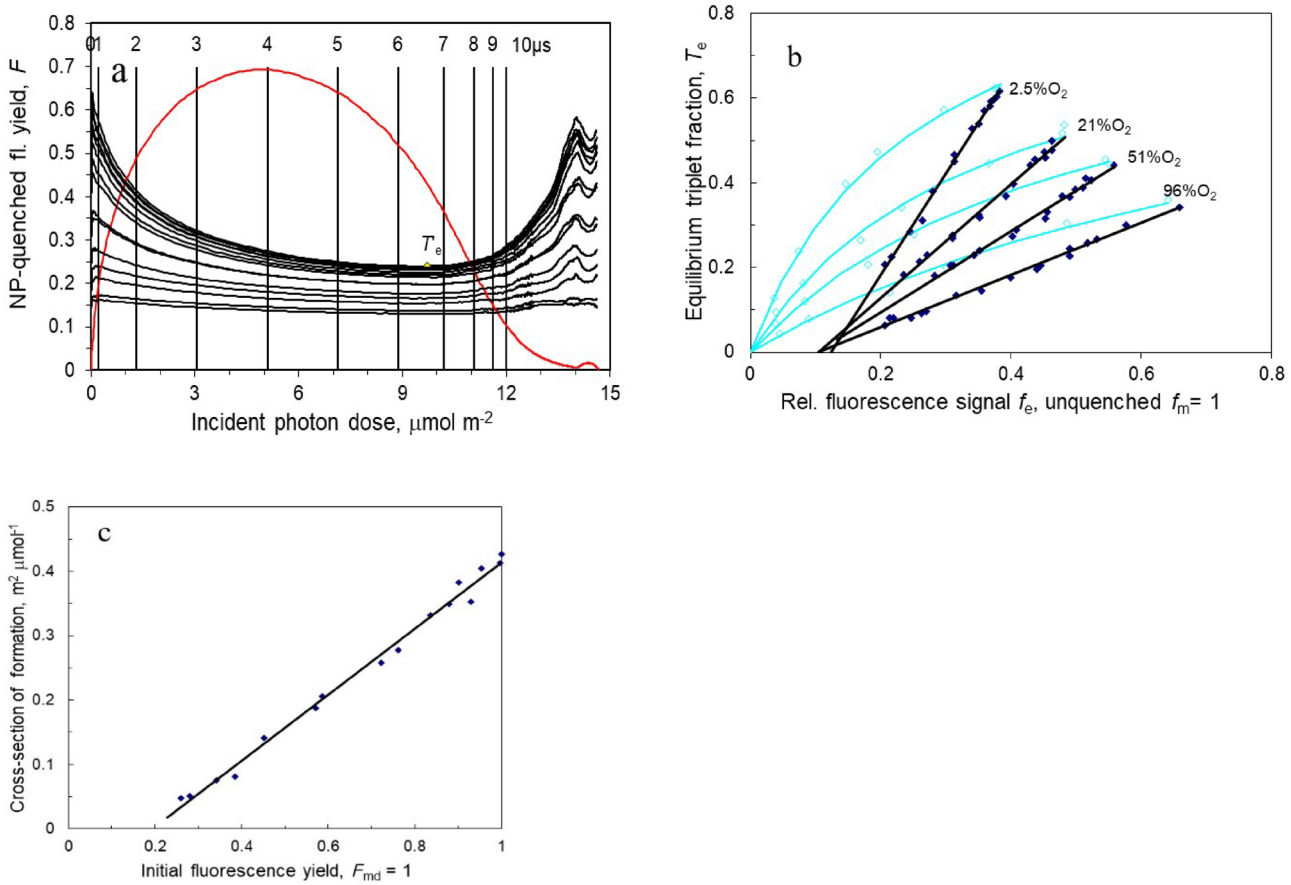

Fig. 5 Triplet formation at different NPQ levels during its relaxation. **a** A sunflower leaf was illuminated for 150 s under 700 µmol m^{-2} s^{-1} of 460 nm light to induce maximum NPQ. Thereafter the actinic light was replaced by 60 µmol m^{-2} s^{-1} of 700 nm background light. F_m pulses (0.3 s) were applied after regular time intervals to monitor relaxation of NPQ. A flash of high power (profile and time shown) was superimposed at the end of each F_m pulse, during which the triplet-quenched fluorescence yield F was monitored (lines in temporal sequence upwards from the bottom). The equilibrium fraction of triplets was calculated as $T_e=(F_m—F_e)/F_m$, where F_m is fluorescence yield in the beginning of the flash and F_e is the minimum yield during the flash. In this example O_2 concentration was 2.5%, CO_2 concentration 150 ppm. **b** Equilibrium triplet fraction during NP-quenched Chl fluorescence in sunflower leaves (black regression lines, filled data points). The experiment of **a** was repeated with different leaves. The equilibrium triplet fraction during flashes is plotted against Chl fluoresence signal f_e at the flash minimum yield F_e (for different leaves, the f signal was normalized to unity at F_{md} in non-quenched state). For comparison, in each leaf the triplet fraction was varied by decreasing flash intensity in the NPQ-off state (light-blue regression lines, empty data points). **c** Initial yield (cross-section) of triplet formation, calculated as the initial slope of the fluorescence traces in **a**, plotted against the initial NP-quenched fluorescence yield

NPQ. The latter method reduces excitation intensity by adjusting the delivery of excitations, while NPQ reduces excitation intensity by limiting the lifetime at a constant delivery rate. The equivalent light intensities, one controlled by photon arrival frequency, the other by lifetime of each excitation, were made comparable via the corresponding Chl fluorescence intensity (not yield).

When plotted against the fluorescence emission signal, f_e, the light-equilibrated triplet fraction, T_e, increased linearly with singlet excitation, as the former increased due to NPQ relaxation. NPQ significantly suppressed triplet formation compared to the same excitation density applied in the unquenched state by properly controlling flash intensity. In the presence of NPQ oxygen still decreased the triplet level. The data of Fig. 5b characterizes the equilibrium pool of accumulated triplets. When triplet formation rate was characterized by the initial slope of the fluorescence trace of Fig. 5a, a similar linear relationship with an offset was obtained (Fig. 5c).

Discussion

Photoprotection is a widely used, multifaceted term whose mechanism is the focus of photosynthesis research now (Bassi and Dall'Osto 2021). Here intentionally

we emphasize one aspect of it, that photoprotection of the photosynthetic machinery is avoidance of singlet oxygen which is formed from ^{3}Chl (Rutherford et al. 2012). Photoprotection therefore is avoidance of excess excitation termination on chlorophyll by transferring the excitation to carotenoid to be terminated there. Mild photoprotection allows the triplet state to be formed on a Car-Chl pair, ending with ^{3}Car. Strong photoprotection is nonphotochemical quenching: excitation is rapidly quenched by the Car-Chl pair with a mechanism not forming the triplet state.

Excitation transfer from Chl to Car has been investigated on isolated subcomplexes of the photosynthetic machinery. Carotenoid triplets with lifetime of about 10 µs were generated in CP47 (Groot et al. 1995) and 6.6 µs in LHCII (Peterman et al. 1997; Gruber et al. 2015). In the latter cited work, which methodically is close to ours, ^{3}Car was generated in a single LHCII trimer by laser pulsing. The observed two-exponential (35 ps and 3.5 ns) fluorescence decay was intuitively understood as fast switching between an annihilation and a non-annihilation regime, corresponding to the presence and absence of a Car triplet state, respectively. Analyzing the data in their Fig. 3 with our model (Eq. 1), we obtained the functional cross-section of triplet formation $a = 0.05$ m^2 µmol^{-1} in isolated LHCII. The value six times smaller than in leaves is caused mainly by the small Chl *a* content of the LHCII trimer compared to the whole PSII antenna. Relating the triplet formation cross-section to the optical absorption cross-section of an individual LHCII of $1.4{\cdot}10^{-15}$ cm$^2 = 0.084$ m^2 µmol^{-1} (Krüger et al. 2010), the ratio of 0.6 results for the quantum yield of triplet formation—like our result in Fig. 4b.

Another interesting result of Gruber et al. (2015) touches on the process of singlet–triplet annihilation. In physics the term means complete destruction of both participants of the process. In our experiments with the green flash the best fit between the model and experiments was obtained setting $b = 1$ (Eq. 4), in agreement with the complete decay of the triplet while annihilating singlet excitation. But while a ^{3}Car triplet was quenching the blue flash, exciting carotenoids directly in experiments of Fig. 1d, the obtained $b/a = 0.4$ showed that the triplet annihilated in less than half of the cases. An extreme was reached under strong laser excitation of Gruber et al. (2015), where the triplet state accumulated in 95% of LHCIIs under excitation density of 80 mol m^{-2} s^{-1}. It means in LHCII the ^{3}Car triplet states did not annihilate while quenching the strong singlet excitation by the 633 nm laser. It seems, the photosynthetic antenna may be a useful model object for further studies of the physics of singlet–triplet annihilation. But major results of our work are related to triplet formation, rather than to their decay.

During photosynthesis in full sunlight in the absence of NPQ, a triplet state would be formed after about every second excitation. However, the triplet lifetime is shorter (microseconds) than the interval between successive excitations (milliseconds) so that at sunlight intensities quenching of Chl fluorescence by annihilation with a triplet state would be minute (Schreiber et al. 2019). Here, to measure the rates of triplet formation and decay, we applied xenon flashes of peak light intensity amounting to moles of photons m^{-2} s^{-1}, accumulating triplet states in a large fraction of PSII complexes—sometimes quenching Chl fluorescence by a half (van Grondelle and Duysens 1980; Paillotin et al. 1983; Gruber et al. 2015; Oja and Laisk 2020). The intrinsic decay time constant of 9 µs (Fig. 2) shows that the triplet states investigated in this work are characteristic of ^{3}Car. Chlorophyll triplet states may be generated in PSII, but their decay is biphasic with lifetimes of 1.6 ms and 6.6 ms (Groot et al. 1994).

Our mathematical analysis of the ^{3}Car budget (Eq. 1) is based on excitonically isolated PSII complexes (Oja and Laisk 2012, 2020). When an antenna containing a Car triplet is excited, the exciting singlet photon is annihilated as soon as the hopping excitation hits the ^{3}Car. On this assumption, only one ^{3}Car may accumulate per PSII. If in a leaf excitation transfer time before annihilation happens to be much longer than the 35 ps in LHCII (Gruber et al. 2015), our reported quantum yield of triplet formation must be increased in proportion with the fraction of residual fluorescence during the annihilation. For example, if the residual fluorescence were 10% of F_{md}, the quantum yield of triplet formation would be 0.73 in Fig. 4b.

The fact that the light curves of equilibrium triplet content (Fig. 1c) are rectangular hyperbolae as predicted by the model ignoring connectivity (Eq. 1), is another proof for the absence of excitonic connectivity between PSII. If excitation lifetime suddenly decreases in a PSII—as happens with ^{3}Car formation—it would absorb excitation from its connected neighbors. The graphs in Fig. 1c would have had a steeper initial slope and faster saturation than the rectangular hyperbolae if PSIIs were excitonically connected. Similarly, if excitation lifetime suddenly increases, as happens after turning NPQ off in a PSII, its connected neighbors still rapidly catch the excitation, causing fluorescence to rise sigmoidally, not linearly, in Fig. 5b. In the absence of connectivity, the widely used Stern–Volmer Law is valid for calculation of the yield of fluorescence in a single PSII unit, because in its antenna different quenchers compete for excitation indeed. Large photosynthetic systems are communities of individual noninteracting photosystem complexes, where the observed global parameters are linear averages based on the proportions of photosystems having alternate properties. The sigmoidal rise of Chl fluorescence during induction is caused by the rising fluorescence yield of Q_A-reduced PSII

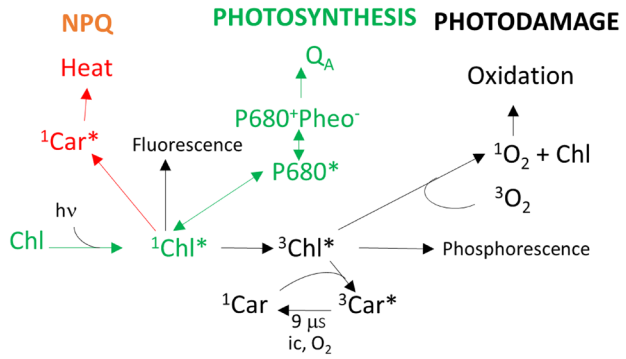

Fig. 6 Schematic depicting of alternative mechanisms of excess excitation dissipation in PSII. When Q_A is photo-reduced formation of the primary radical pair $P680^+Pheo^-$ is hindered. Consequent accumulation of excited singlet chlorophyll ($^1Chl^*$) terminates in the $^3Chl^*$ triplet state, which reacts with atmospheric $^3O_2$ to form singlet oxygen ($^1O_2$) and ^1Chl. This deleterious scenario is prevented by fast transfer of $^3Chl^*$ to a carotenoid, $^3Car^*$, where the triplet state decays by intersystem crossing (ic) in 9 µs. Photoprotection is enhanced by nonphotochemical quenching, NPQ, which transfers excitation from $^1Chl^*$ to $^1Car^*$ in competition with photosynthesis

units (Oja and Laisk 2012, 2020; Laisk and Oja 2020; Sipka et al. 2021, 2022).

The strict equality of the growth of the triplet-forming and diminution of the quenching fractions of PSII during relaxation of q_E (Fig. 5b,c) indicates that one and the same PSII is switched between the triplet-forming and NP-quenching modes without "lake-type" excitation transfer between PSII units (Ruban et al. 2012; Belgio et al. 2014; Liguori et al. 2015). The offset of the graphs on the fluorescence axis is consistent with the model that one and the same Car-Chl site is switching between the triplet-forming and quenching modes. If *distinct* Car-Chl sites for triplet formation and NPQ were to compete for excitation in an individual PSII then the rate constant for triplet formation (k_T) would remain constant even as the rate constant for NPQ (k_N) varied. Hence, the yields of triplet formation T and fluorescence emission F would be related as $T = k_T/(k_F + k_T + k_N)$ and $F = k_F/(k_F + k_T + k_N)$. Furthermore, the ratio $T/F = k_T/k_F$ would be constant for all k_N values. Thus the black lines in Figs. 5b and c would approach zero without an offset. By contrast, the clear presence of an offset means that k_T is not fixed leading us to reject the separate site hypothesis.

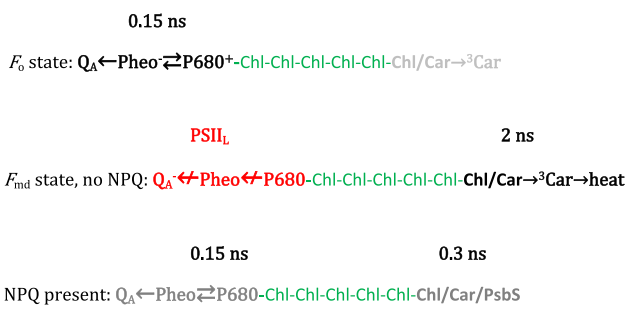

Box 1 Schemes of excitation quenching in PSII. -Chl-Chl- illustrates the antenna, and approximate excitation termination times are indicated. Dominating pathways are shown in bold shades of grey

The scheme of Box 1 illustrates the following model of PSII excitation. Under low light when Q_A is oxidized, the $Pheo^-P680^+$ radical pair traps antenna excitation, by far outcompeting other excitation terminators. At higher light intensities, when Q_A becomes reduced, protein conformation changes in the PSII reaction center, turning it into the light-adapted, charge-separated $PSII_L$ state (Sipka et al. 2021, 2022). In this PSII state excitation is detained in the antenna—with the prospect of being terminated via ^3Chl and consequent $^1O_2$ formation. To outcompete this detrimental prospect, a Car-Chl pigment pair traps the excitation within 1–2 ns into ^3Car, allowing for a lowering of fluorescence yield. The presence of the $PSII_L$ state under light saturation of photosynthesis could be the primary alarm signal to improve photoprotection by inducing NPQ, but presently we only know other, inertial signal mediators like transmembrane proton gradient, zeaxanthin and PsbS, come into play in the NPQ induction process (Bassi and Dall'Osto 2021), somehow switching the triplet-forming Car-Chl site into the q_E singlet-quenching mode (Mascoli et al. 2019).

The basis for the model of Fig. 6 and Box. 1 is the microseconds rise of Chl fluorescence from F_o to F_f (Oja and Laisk 2020), seen also in Fig. 3 of this work. Recently it has been shown that following Q_A reduction, a protein conformation change in the PSII reaction center is induced by recurring formation and recombination of the primary $Pheo^-P680^+$ radical pair (Sipka et al. 2019, 2021, 2022; Magyar et al. 2022). We propose that the so obtained conformation-dependent $PSII_L$ state, as defined by these authors, underlies Chl fluorescence increases to the F_f or F_{md} state. The flash-induced, F_f, and saturation pulse-induced, F_{md}, fluorescence yields are still enigmatic. Relevant to the present work is the fact that excitation is terminated by ^3Car formation in both states (Oja and Laisk 2020 and Fig. 3 of this work), though fluorescence yield (excitation lifetime) is almost by a half lower in the F_f state compared to the F_{md} state. As Q_A reduction induces F_f but both Q_A and Q_B need to be reduced in the F_{md} fluorescence state (Prášil et al. 2018; Laisk and Oja 2020), it means the speed of the excitation terminating ^3Car formation in the antenna is tightly controlled by reduction state of the reaction center (Farooq et al. 2018). There are weighty arguments in favor of LHCII as the most likely site of the Car-Chl pair in the quenching state (Liguori et al. 2015; Ruban and Wilson 2020), with the caveat of 30–40% NPQ occurring in the minor antenna and in the PSII core (Nicol et al. 2021).

A hindrance in NPQ investigations has been the deceptive multiplicity of the investigation object: similar Car-Chl

structures have been found in different subcomplexes of the PSII antenna. Isolated LHCII, as well as other subcomplexes, can be turned into quenching states (Ruban 2016; Xu et al. 2015). Different mechanisms have been suggested to explain it, like interactions between Chls (Miloslavina et al. 2008; Müller et al. 2010), energy/electron transfer between Chl and xanthophyll (Ruban et al. 2007; Ahn et al. 2008), excitonic mixing of Chl and Xan (van Amerongen and van Grondelle 2001; Bode et al. 2009), and formation of a radical cation between zeaxanthin and lutein (Dall'Osto et al. 2017). Such diversity has, at least partly, been abetted by contradictions in understanding the role of carotenoids as accessory pigments harvesting light for photosynthesis. In isolated antenna subcomplexes, most of the excitation energy transfer occurs from the Car S_2 to Chl *b* (Croce et al. 2001), but there have been reports about energy transfer from the Car S_1 excitation level to Chl *a* (Walla et al. 2002). In intact leaves and green algae, the "accessory" role of carotenoids in photosynthesis is not light harvesting but rather the opposite. About 30% of blue light energy is shielded by carotenoids from entering photosynthesis. A large part of excitation absorbed by carotenoids is not transferred to the photochemical center but is largely quenched (Emerson and Lewis 1942, 1943; Laisk et al. 2014).

The functional task of carotenoids thus is to absorb ^{3}Chl triplet states and to non-photochemically quench excessive excitation (Ruban et al. 2007; Mascoli et al. 2019; Agostini et al. 2021). The ability to quench excitation seems unnecessary for each individual Lhcb monomer, but this is so only while the subunit is assembled into the antenna, rapidly transferring excitation. There are occasions when a subunit is isolated. For example, it may happen before the freshly synthesized monomers have been assembled into the light-harvesting trimer and before the latter is assembled with the core antenna (Cutolo et al. 2023). And there is the state transition type regulation, where an LHCII unit is transferred between PSII and PSI, isolated from both photosystems (Allen 2003). For such cases the quenching mechanism is a safeguard preventing destruction of the temporarily detached pigment protein by singlet oxygen.

Now about the necessity for the two-step photoprotection mechanism. Transformation of the ^{3}Car state to form $^1O_2$ is considered impossible because of the inadequate energy of the carotenoid triplet state. The lowest triplet level of ^{3}Chl *a* is 1.31 eV (10,500 cm^{-1}) higher than the singlet ground level: 973 nm phosphorescence is emitted when ^{3}Chl relaxes to ^{1}Chl. In carotenoids of LHCII, the triplet level is only 0.75 eV (about 6000 cm^{-1}) higher than the singlet ground level: the phosphorescence wavelength is 1702 nm. Singlet O_2 relaxes to the ground $^3O_2$ state emitting phosphorescence at 1270 nm, indicating an energy difference 1 eV. Thanks to this energy difference, carotenoids are believed to be safe protectors against singlet O_2 formation in the photosynthetic machinery (Siefermann-Harms 1987; Telfer 2014).

Notwithstanding this protection mechanism, at atmospheric concentration, O_2 significantly enhances quenching of ^{3}Car states: in our experiments at 100% O_2 their decay rate was six times faster than the intrinsic rate in the absence of oxygen. This paradox is resolved by suggesting enhanced intersystem crossing of ^{3}Car to the ground singlet state in the presence of the paramagnetic oxygen (Ho et al. 2017). Nevertheless, $^1O_2$ is produced in isolated PSII membranes (Vass et al. 1992; Telfer 2014; Krieger-Liszkay 2005), and recently has been intensely studied in intact plants (Dmitrieva et al. 2020). Though its most likely production site is the PSII reaction center (Mattila et al. 2023), the special way that the ^{3}Chl and ^{3}Car wavefunctions are shared in plants may provide a chance for a $^3O_2$ molecule to interfere while the triplet state is transferred from ^{3}Chl to ^{3}Car (Gall et al. 2011): some $^1O_2$ is formed in isolated monomeric Lhcb5 subcomplexes indeed (Ballottari et al. 2013). This could be the biological reason why the dual photoprotection mechanism has been developed in evolution: the $^3\text{Chl} \rightarrow {}^3\text{Car}$ triplet transfer provides incomplete protection, which is elaborated into perfect q_E-protection by internal conversion via the Car S_1 (or S*) excitation level.

Such an integrated approach like the present work, carried out on intact leaves, provides information about in vivo kinetics of the in vitro processes studied, painting a picture of the whole process of excitation energy transfer and quenching in photosynthesis. But the integral approach cannot resolve the mechanisms. It remains to be investigated in vitro, what happens in the PSII reaction center during microseconds after electron transfer to Q_A? What is the physical difference between the triplet-forming and q_E quenching states of the photoprotective Car-Chl pair and how are xanthophylls and PsbS protein related to the transformation?

Acknowledgements Lettuce was a gift by R. Külasepp and E. Feldmann from Grüne Fee Tartu. The LeCroy oscilloscope was made available by prof. A. Aabloo, Tartu University.

Author contributions AL planned experiments, interpreted results and wrote the text.RP interpreted results and wrote the text.VO Carried out experiments and interpreted results.

Funding The project was financed by University of Tartu, Institute of Technology (basic funding), and by Estonian Academy of Science (A.L.).

Data availability Not applicable.

Declarations

Conflict of interest The authors had no conflict of interest.

References

Agostini A, Nicol L, Da Roit N, Bortolus M, Croce R, Carbonera D (2021) Altering the exciton landscape by removal of specific chlorophylls in monomeric LHCII provides information on the sites of triplet formation and quenching by means of ODMR and EPR spectroscopies. BBA Bioenergetics 1862:148481

Ahn TK, Avenson TJ, Ballottari M, Cheng Y-C, Niyogi KK, Bassi R, Fleming GR (2008) Architecture of a charge-transfer state regulating light harvesting in a plant antenna protein. Science 320:794–797

Allen JF (2003) State transition—a question of balance. Science 299:1530–1532

Ballottari M, Mozzo M, Girardon J, Hienerwadel R, Bassi R (2013) Chlorophyll triplet quenching and photoprotection in the higher plant monomeric antenna protein Lhcb5. J Phys Chem B 117:11337–11348. https://doi.org/10.1021/jp402977y

Bassi R, Dall'Osto L (2021) Dissipation of light energy absorbed in excess: the molecular mechanisms. Annu Rev Plant Biol 72:47–76

Belgio E, Johnson MP, Jurić S, Ruban AV (2012) Higher plant photosystem II light-harvesting antenna, not the reaction center, determines the excited-state lifetime—both the maximum and the nonphotochemically quenched. Biophys J 102:2761–2771

Belgio E, Kapitonova E, Chmeliov J, Duffy CDP, Ungerer P, Valkunas L, Ruban AV (2014) Economic photoprotection in photosystem II that retains a complete light-harvesting system with slow energy traps. Nat Commun 5:4433

Bode S, Quentmeier CC, Liao PN, Hafi N, Barros T, Wilk L, Bittner F, Walla PJ (2009) On the regulation of photosynthesis by excitonic interactions between carotenoids and chlorophylls. Proc Natl Acad Sci USA 106:12311–12316

Bowers PG, Porter G (1967) Quantum yields of triplet formation in solutions of chlorophyll. Proc R Soc A 296:435–441

Christen G, Reifarth F, Renger G (1998) On the origin of the '35-µs kinetics' of $P680^{+\bullet}$ reduction in photosystem II with an intact water oxidizing complex. FEBS Lett 429:49–52

Chukhutsina VU, Holzwarth AR, Croce R (2019) Time-resolved fluorescence measurements on leaves: principles and recent developments. Photosynth Res 140:355–369

Croce R, Müller MG, Bassi R, Holzwarth AR (2001) Carotenoid-to-chlorophyll energy transfer in recombinant major light-harvesting complex (LHCII) of higher plants: I—femtosecond transient absorption measurements. Biophys J 80:901–915

Cutolo EA, Guardini Z, Dall'Osto L, Bassi R (2023) Tansley review: a paler shade of green: engineering cellular chlorophyll content to enhance photosynthesis in crowded environments. New Phytol 239:1567–1583

DallOsto L, Cazzaniga S, Bressan M, Paleček D, Židek K, Niyogi KK, Fleming GR, Zigmantas D, Bassi R (2017) Two mechanisms for dissipation of excess light in monomeric and trimeric light-harvesting complexes. Nat Plants 3:1–9. https://doi.org/10.1038/nplants.2017.33

Dmitrieva VA, Tyutereva EV, Voitsekhovskaja OV (2020) Singlet oxygen in plants: generation, detection, and signaling roles. Int J Mol Sci 21:3237. https://doi.org/10.3390/ijms21093237

Emerson R, Lewis CR (1942) The photosynthetic efficiency of phycocyanin in *Chroococcus*, and the problem of carotenoid participation in photosynthesis. J Gen Physiol 20:579–595

Emerson R, Lewis CM (1943) The dependence of quantum yield of *Chlorella* photosynthesis on wave length of light. Am J Bot 30:165–178

Farooq S, Chmeliov J, Wientjes E, Koehorst R, Bader A, Valkunas L, Trinkunas G, van Amerongen H (2018) Dynamic feedback of the photosystem II reaction centre on photoprotection in plants. Nat Plants 4:225–231

Gall A, Berera R, Alexandre MTA, Pascal AA, Bordes L, Mendes-Pinto MM, Andrianambinintsoa S, Stoitchkova KV, Marin A, Valkunas L, Horton P, Kennis JTM, van Grondelle R, Ruban A, Robert B (2011) Molecular adaptation of photoprotection: triplet states in light-harvesting proteins. Biophys J 101:934–942

Golbeck JH (1987) Structure, function and organization of the photosystem I reaction centre complex. Biochim Biophys Acta 895:167–204

Groot M-L, Peterman JG, van Kan PJM, van Stokkum IHM, Dekker JP, van Grondelle R (1994) Temperature-dependent triplet and fluorescence quantum yields of the photosystem II reaction center described in a thermodynamic model. Biophysical J 67:318–330

Groot M-L, Peterman EJG, van Stokkum IHM, Dekker JP, van Grondelle R (1995) Triplet and fluorescing states of the CP47 antenna complex of photosystem II studied as a function of temperature. Biophysical J 68:281–290

Gruber JM, Chmeliov J, Krüger TPJ, Valkunas L, van Grondelle R (2015) Singlet–triplet annihilation in single LHCII complexes. Phys Chem Chem Phys 17:19844–19853

Ho J, Kish E, Méndez-Hernández DD, WongCarter K, Pillai S, Kodis G, Niklas J, Poluektov OG, Gust D, Moore TA, Moore AL, Batista VS, Robert B (2017) Triplet–triplet energy transfer in artificial and natural photosynthetic antennas. Proc Natl Acad Sci USA 114:E5513–E5521

Holzwarth AR, Miloslavina Y, Nilkens M, Jahns P (2009) Identification of two quenching sites active in the regulation of photosynthetic light-harvesting. Chem Phys Lett 483:262–267

Kaplanova M, Parma L (1984) Effect of excitation and emission wavelength on the fluorescence lifetimes of chlorophyll a. Gen Physiol Biophys 3:127–134

Krieger-Liszkay A (2005) Singlet oxygen production in photosynthesis. J Exp Bot 56(411):337–346

Krüger TPJ, Novoderezhkin VI, Ilioaia C, van Grondelle R (2010) Fluorescence spectral dynamics of single LHCII trimers. Biophys J 98:3093–3101

Laisk A, Oja V (1998) Dynamics of Leaf Photosynthesis: rapid-response measurements and their interpretations. CSIRO, Collingwood

Laisk A, Oja V (2020) Variable fluorescence of closed photochemical reaction centers. Photosyth Res 143:335–346. https://doi.org/10.1007/s11120-020-00712-3

Laisk A, Oja V, Rasulov B, Rämma H, Eichelmann H, Kasparova I, Pettai H, Padu E, Vapaavuori E (2002) A computer-operated routine of gas exchange and optical measurements to diagnose photosynthetic apparatus in leaves. Plant Cell Env 25:923–943

Laisk A, Eichelmann H, Oja V, Talts E, Scheibe R (2007) Rates and roles of cyclic and alternative electron flow in potato leaves. Plant Cell Physiol 48(11):1575–1588

Laisk A, Talts E, Oja V, Eichelmann H, Peterson R (2010) Fast cyclic electron transport around photosystem I in leaves under far-red light: a proton-uncoupled pathway? Photosynth Res 103:79–95

Laisk A, Eichelmann H, Oja V (2012) Oxygen evolution and chlorophyll fluorescence from multiple turnover light pulses: charge recombination in photosystem II in sunflower leaves. Photosynth Res 113:145–155

Laisk A, Oja V, Eichelmann H, Dall'Osto L (2014) Action spectra of photosystems II and I and quantum yield of photosynthesis in leaves in State 1. Biochim Biophys Acta 1837:315–325

Laisk A, Oja V, Eichelmann H (2016) Kinetics of plastoquinol oxidation by the Q-cycle in leaves. Biochim Biophys Acta 1857:819–830

Liguori N, Periole X, Marrink SJ, Croce R (2015) From light-harvesting to photoprotection: structural basis of the dynamic switch of the major antenna complex of plants (LHCII). Sci Rep 5:15661. https://doi.org/10.1038/srep15661

Magyar M, Akhtar P, Sipka G, Han W, Li X, Han G, Shen J-R, Lambrev PH, Garab G (2022) Dependence of the rate-limiting steps in the dark-to-light transition of photosystem II on the lipidic environment of the reaction center. Photosynthetica 60:147–156

Mascoli V, Liguori N, Xu P, Roy LM, van Stokkum IHM, Croce R (2019) Capturing the quenching mechanism of light-harvesting complexes of plants by zooming in on the ensemble. Chemistry 5:2900–2912

Mathis P, Butler WL, Satoh K (1979) Carotenoid triplet state and chlorophyll fluorescence quenching in chloroplasts and subchloroplast particles. Photochem Photobiol 30:603–614

Mattila H, Mishra S, Tyystjärvi T, Tyystjärvi E (2023) Singlet oxygen production by photosystem II is caused by misses of the oxygen evolving complex. New Phytol 237:113–125

Miloslavina Y, Wehner A, Lambrev PH, Wientjes E, Reus M, Garab G, Croce R, Holzwarth AR (2008) Far-red fluorescence: a direct spectroscopic marker for LHCII oligomer formation in non-photochemical quenching. FEBS Lett 582:3625–3631

Müller MG, Lambrev P, Reus M, Wientjes E, Croce R, Holzwarth AR (2010) Singlet energy dissipation in the photosystem II light-harvesting complex does not involve energy transfer to carotenoids. Chem Phys Chem 11:1289–1296

Nicol L, Mascoli V, van Amerongen H, Croce R (2021) The quantitative contribution of different photosystem II compartments to non-photochemical quenching in Arabidopsis. bioRxiv preprint https://doi.org/10.1101/2021.10.17.463719:1-23

Oja V, Laisk A (2000) Oxygen yield from single turnover flashes in leaves:non-photochemical excitation quenching and the number of active PSII. Biochim Biophys Acta 1460(2–3):291–301

Oja V, Laisk A (2012) Photosystem II antennae are not energetically connected: evidence based on flash-induced O_2 evolution and chlorophyll fluorescence in sunflower leaves. Photosynth Res 114:15–28

Oja V, Laisk A (2020) Time- and reduction-dependent rise of photosystem II fluorescence during microseconds-long inductions in leaves. Photosynth Res. 145: 209–225 https://doi.org/10.1007/s11120-020-00783-2

Oja V, Eichelmann H, Anijalg A, Rämma H, Laisk A (2010) Equilibrium or disequilibrium? A dual-wavelength investigation of photosystem I donors. Photosynth Res 103:153–166. https://doi.org/10.1007/s11120-010-9534-z

Oja V, Eichelmann H, Laisk A (2011) Oxygen evolution from single- and multiple-turnover light pulses: temporal kinetics of electron transport through PSII in sunflower leaves. Photosynth Res 110:99–109

Paillotin G, Geactinov NE, Breton J (1983) A master equation theory of fluorescence induction, photochemical yield, and singlet-triplet exciton quenching in photosynthetic systems. Biophys J 44:65–77

Pascal AA, Liu Z, Broess K, van Oort B, van Amerongen H, Wang C, Horton P, Robert B, Chang W, Ruban A (2005) Molecular basis of photoprotection and control of photosynthetic light harvesting. Nature 436:134–137. https://doi.org/10.1038/nature03795

Peterman EJG, Gradinaru CC, Calkoen F, Borst JC, van Grondelle R, van Amerongen H (1997) Xanthophylls in light-harvesting complex II of higher plants: lght hrvesting and tiplet qenching. Biochemistry 36:12208–12215

Prášil O, Kolber ZS, Falkowski PG (2018) Control of the maximal chlorophyll fluorescence yield by the Q_B binding site. Photosynthetica 56:150–162

Ruban AV (2016) Nonphotochemical chlorophyll fluorescence quenching: Mechanism and effectiveness in protecting plants from photodamage. Plant Physiol 170:1903–1916

Ruban AV, Wilson S (2020) The mechanism of non-photochemical quenching in plants: localization and driving forces. Plant Cell Physiol 62:1063–1072

Ruban AV, Berera R, Ilioaia C, van Stokkum IHM, Kennis JTM, Pascal AA, van Amerongen H, Robert B, Horton P, van Grondelle R (2007) Identification of a mechanism of photoprotective energy dissipation in higher plants. Nature 450:575–578

Ruban AV, Johnson MP, Duffy CDP (2012) The photoprotective molecular switch in the photosystem II antenna. Biochim Biophys Acta 1817:167–181

Rutherford AW, Osyczka A, Rappaport F (2012) Back-reactions, short-circuits, leaks and other energy wasteful reactions in biological electron transfer: redox tuning to survive life in O_2. FEBS Lett 586:603–616

Rutkauskas D, Chmeliov J, Johnson M, Ruban A, Valkunas L (2012) Exciton annihilation as a probe of the light-harvesting antenna transition into the photoprotective mode. Chem Phys 404:123–128

Schödel R, Irrgang K-D, Voigt J, Renger G (1999) Quenching of chlorophyll fluorescence by triplets in solubilized light-harvesting complex II (LHCII). Biophysical J 76:2238–2248

Schreiber U (2023) Light-induced changes of far-red excited chlorophyll fluorescence: further evidence for variable fluorescence of photosystem I in vivo. Photosynthesis Res 155:247–270

Schreiber U, Klughammer C, Schansker G (2019) Rapidly reversible chlorophyll fluorescence quenching induced by pulses of supersaturating light in vivo. Photosynth Res 142:35–50

Siefermann-Harms D (1987) The light-harvesting and protective functions of carotenoids in photosynthetic membranes. Physiol Plantarum 69:561–568

Sipka G, Müller P, Brettel K, Magyar M, Kovács L, Zhu Q, Xiao Y, Han G, Lambrev PH, Shen J-R, Garab G (2019) Redox transients of P680 associated with the incremental chlorophyll-a fluorescence yield rises elicited by a series of saturating flashes in diuron-treated photosystem II core complex of *Thermosynechococcus vulcanus*. Physiol Plantarum 166:22–32

Sipka G, Magyar M, Mezzetti A, Parveen A, Zhu Q, Xiao Y, Han G, Santabarbara S, Shen J-R, Lambrev PH, Garab G (2021) Light-adapted charge-separated state of photosystem II: structural and functional dynamics of the closed reaction center. Plant Cell 33:1286–1302. https://doi.org/10.1093/plcell/koab1008

Sipka G, Nagy L, Magyar M, Akhtar P, Shen J-R, Holzwarth AR, Lambrev PH, Garab G (2022) Light-induced reversible reorganizations in closed Type II reaction centre complexes: physiological roles and physical mechanisms. Open Biol 12:220297. https://doi.org/10.1098/rsob.220297

Telfer A (2014) Singlet oxygen production by PSII under light stress: mechanism, detection and the protective role of b-arotene. Plant Cell Physiol 55:1216–1223

van Amerongen H, van Grondelle R (2001) Understanding the energy transfer function of LHCII, the major light-harvesting complex of plants. J Phys Chem B 105:604–617

van Grondelle R, Duysens LN (1980) On the quenching of the fluorescence yield in photosynthetic systems. Plant Physiol 65:751–754

Vass I, Styring S, Hundal T, Koivuniemi A, Aro E-M, Andersson B (1992) Reversible and irreversible intermediates during photoinhibition of photosystem II: stable reduced Q_A species promote chlorophyll triplet formation. Proc Natl Acad Sci USA 89:1408–1412

Walla PJ, Yom J, Krueger BP, Fleming GR (2000) Two-photon excitation spectrum of light-harvesting complex II and fluorescence upconversion after one- and two-photon excitation of the carotenoids. J Phys Chem B 104:4799–4806

Walla PJ, Linden PA, Ohta K, Fleming GR (2002) Excited-state kinetics of the carotenoid S_1 State in LHC II and two-photon excitation spectra of lutein and β-carotene in solution: efficient Car $S_1 \rightarrow$Chl electronic energy transfer via hot S_1 states? J Phys Chem A 106:1909–1916

Xu P, Tian L, Kloz M, Croce R (2015) Molecular insights into Zeaxanthin-dependent quenching in higher plants. Sci Rep 5:13679. https://doi.org/10.1038/srep13679